Thermal preparation and characterization of nanodispersed copper-containing powders produced by non-equilibrium electrochemical oxidation of metals

Valeriy V. Korobochkin[a], Johannes H. Potgieter[b,c*], Natalia V. Usoltseva[a], Alesya S. Dolinina[a], Vladimir V. An[a]

[a] *Kizhner Research Center, School of Advanced Manufacturing Technologies, Tomsk Polytechnic University, Lenin avenue, 30, Tomsk, 634050, Russia*

[b] *Department of Natural Sciences, Manchester Metropolitan University, Manchester, M15 6GD, UK*

[*] *corresponding author, h.potgeiter@mmu.ac.uk*

[c] *School of Chemical and Metallurgical Engineering, University of the Witwatersrand, Private Bag X3, Wits, 2050, South Africa*

ABSTRACT

Physicochemical properties of copper, aluminum and cadmium oxides determine their application in different ways. Electrochemical metal oxidation using alternating current (AC) influences the band gap of prepared copper-containing oxide materials and result in a blue shift. The use of alternating current provides sufficient conditions responsible for nanosized materials formation (grain size: 20–30 nm for separate copper oxidation, 15–20 nm for joint copper and aluminum oxidation). In the present work, XRD and DSC/DTG, SEM analyses were used to characterize the electrolysis products. A decrease of the thermal transformation temperature (Cu_2O oxidation at 260 °C, copper-aluminum layered double hydroxide (Cu-Al/LDH) decomposition at 140 °C) of the products of both separate copper oxidation and joint copper and aluminum (or cadmium) oxidation was established when compared with those of the same oxides prepared by the usual methods. Solution aging of these products after joint electrochemical oxidation of copper and aluminum results in the transformation of Cu_2O-AlOOH to Cu-Al/LDH. Products of the joint oxidation of copper and cadmium consist of oxides and hydroxides of copper and cadmium (γ-$Cd(OH)_2$, $Cu(OH)_2$, β-$Cd(OH)_2$, CdO and Cu_2O), which are not capable to form LDH. The synthesized copper-containing mixed metal oxide will be investigated elsewhere to obtain their structural characterization and operating performance in catalytic, photocatalytic and other applications.

Key words: electrolysis, phase composition, DSC analysis, copper oxides, aluminum oxide, cadmium oxide

1. Introduction

Metal oxides are the largest part of powdered nanomaterials. Among the methods to obtain functional metal oxide materials, those of special interest include non-equilibrium pathways, like self-propagating, high-temperature synthesis, mechanochemical, plasma-chemical syntheses, electrical explosion of wires, electrospark erosion method, and electrochemical methods [1-6]. It is due to the defective structure and high internal energy storage of such materials, which cause high reactivity to phase transformations of metal oxides and their use in various processes.

Most of the existing electrochemical methods produce coatings of metal oxides [7, 8], mixed oxides in solutions [9], layered double hydroxides (LDH)[10] and perovskites [11]. Alternating current electrolysis provides a route to the synthesis of metal oxides powders at non-equilibrium conditions. Non-equilibrium electrolysis forms metal oxides [12] and oxide systems [13, 14] with high dispersion, developed pore structures and a low content of impurities.

The copper-containing oxide systems are widely used as both solid materials and suspensions. The copper-cadmium system is used as an active mass of chemical energy for battery production, as a component of semiconductor materials and luminophors, as well as in homeopathic medicine such as anticancer drugs [15-17]. The copper-aluminum oxide system is also of current interest. It is used as oxygen carrier in chemical looping combustion [18], as a catalyst in organic synthesis [19, 20], the catalytic [21, 22] and electrocatalytic [23, 24] treatment of industrial wastes, and simultaneous purification of flue gases consisting of SO_2 and NO_x emissions [25].

Semiconductor metal oxide nanomaterials can be used as photoelectrodes (photoanodes and photocathodes) for photoelectrochemical solar water splitting in a photoelectrochemical cell for converting solar energy to hydrogen fuel conversion [26]. The Cu_2O/CuO heterojunction structure is an effective photocathode for photoelectrochemical water reduction and shows improved stability compared to some other combinations [27]. The CdO-based heterostructure is used as a photoanode for photoelectrochemical water oxidation [28].

Adding nanoparticles (metal, metal oxides, carbon based and other conductive compounds) in a fluid produce a nanofluid with enhanced thermal performance [26, 29-37]. The reasons for the enhancing of the thermal conductivity of nanofluids are, amongst others [38]: increased surface area, intensification of interaction between liquid and particles, intensification of the fluid's turbulence and mixing, and a more uniform temperature distribution in the fluid.

Nanofluids are considered promising to carry out processes that depend on thermal conductivity of a fluid. Nanofluids can be utilized in concentrating solar collectors to increase their efficiency of absorption and conversion of solar energy due to faster heat dissipation [32–35, 39]. They have effective heat transfer applications as a heating agent in heat exchangers [40] or cooling medium in refrigerators [38]. Adding nanoparticles in solar stills enhance the distillate (freshwater) productivity by the solar water heating systems [30, 36]. It is due to the increase of fluid thermal conductivity, and consequently faster evaporation. According to a review [30], even very low concentrations of nanoparticles (hundredths, tenths or a few of percent) increased the productivity by several up to one hundred percent.

Among different water-based nanofluids of metal oxides, nanofluids of CuO and Al_2O_3 nanoparticles possess the highest relative thermal conductivity coefficient [41, 42]. Thermal conductivity of water-based CuO-Al_2O_3 hybrid nanofluids is higher than thermal conductivity of water-based nanofluids of either CuO or Al_2O_3 [43]. CdO nanofluid is also reported [44] to enhance the heat transfer rate of heat exchangers.

It is known that nanomaterial particle sizes are correlated with physical parameters (e.g. the size of magnetic domains, the mean free path of electrons, de Broglie wavelength, the size of excitons in semiconductors, etc.) that determine the mechanical, optical, and electrical properties of the system. Furthermore, the reduction of particle size causes an increase of surface atoms possessing features of the surface states. At the same time, the production method determines not only the size and shape of a particle, but also the surface energy. It affects the material's characteristics, particularly the temperature of any phase transformation. Usually, small particle size nanomaterials have an increased internal energy storage, which result in high reactivity that can lead to temperature decreases of redox processes and structural ordering.

Different methods of analysis (XRD, DTA/DSC analysis and others) are used to characterize the synthesized oxides. The choice depends on the required information. X-ray diffraction provides information on phase compositions and coherent scattering regions, while DTA/DSC analysis reveals the temperatures of thermal transformations [45]. Thermal analysis methods for bulk materials are not necessarily applicable to nanoparticles, because of specific properties of matter at the nanoscale level [46].

The work reported here aims to characterize the mixed copper-containing oxides produced by alternating current electrolysis. Another unique aspect of this work lies in the demonstration that a non-equilibrium electrochemical oxidation technique can be employed for designing novel nanostructured copper-containing materials, which can be successfully used in different catalytic and photocatalytic applications, especially green energy technologies. The objective is to illustrate that the applicability of nanomaterials can be predicted on the basis of their composition, as well as the thermal performance of both the solid nanostructured products of electrolysis and their suspension in working fluids. Nanoparticles or nanostructured materials that can be obtained by AC electrolysis seem to be able to improve the catalytic properties of metal oxides and the conductive properties of hybrid metal oxide nanofluids due to their high specific surface area which improves mass and heat transfer.

2. Experimental section

2.1. Materials and methods

Sodium chloride was purchased and directly used as received without further purification. Sheets of copper, aluminum and cadmium were used to prepare soluble electrodes.

X-ray diffraction (XRD) measurements were performed using a DRON-3M diffractometer (CuK_α radiation, λ=1.5418 Å) at 25 mA and 35 kV. The data were collected from 10 to 70° 2 θ at a counting rate of 4 θ/min. PDF 2 database was used to identify the phase composition. Full-profile analysis of X-ray diffraction patterns was performed with the program "Powder Cell 2.4" to determine the content of copper compounds in the samples and the crystallite size (coherent scattering region).

Thermogravimetric analysis (TGA) and differential scanning calorimetry (DSC) were carried out on a thermal analyzer SDT Q600 in air at a heating rate of 10°C min^{-1} in the temperature range from ambient to 600 °C (copper oxide, copper-aluminum oxide) and 1000 °C (copper-cadmium oxide).

2.2. Synthesis of copper-containing powders

Two different metal plates (copper and aluminum or copper and cadmium) were jointly electrochemically oxidized. The densities of alternating current of industrial frequency (50 Hz) was 0.5 – 3.0 A/cm^2. Electrochemical oxidation was carried out in a 3 wt % sodium chloride solution, based on the concentration dependence of the metal oxidation rate and energy consumption. Copper, aluminum and cadmium plates were used as soluble electrodes. Metal oxidation rates reach a peak at 90 °C (Cu and Al oxidation) and 100 °C (Cu and Cd oxidation).

3. Results and discussion

3.1. Electrochemical copper oxidation

To avoid changing the phase composition, the product of electrochemical copper oxidation was dried at the residual pressure of 3–5 kPa without prior washing. The drying duration depended on the amount of water in suspension. Our samples were dried for two hours. Drying at the residual pressure of 3−5 kPa should be carried out until the sample became free-flowing. Following drying until the end of the weight change period can be done at atmospheric pressure.

According to the XRD analysis, the powder consists of copper (I) oxide and sodium chloride electrolyte (Fig. 1). Cu_2O crystallizes in a cubic crystal system, space group Pn3m. It is known [47] that the shape of XRD peaks indicates the phase crystallinity. XRD peaks of this copper (I) oxide are narrow, have high intensity and distinct maxima. Hence, the copper (I) oxide formed after the electrochemical copper oxidation is highly crystalline.

In contrast to the red copper (I) oxide produced by conventional methods, a yellow product is formed by AC electrolysis. Cu_2O is a p-type metal oxide semiconductor. Its band gap of 2.2 eV becomes greater with the decrease of nanoparticle size. The change of powder color is caused by a shift of the fundamental absorption edge towards the higher energies (blue shift) due to the increase of the band gap [48, 49]. This is an example of how the properties of the materials can change because of their nanostructural nature.

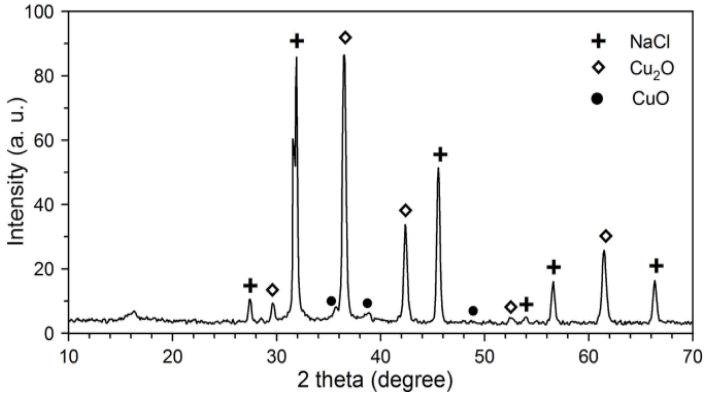

Fig. 1. XRD pattern of the product of AC electrochemical copper oxidation in a 3 wt % solution of sodium chloride at a current density of 1 A/cm^2

Copper (I) oxide is oxidized after heat treatment in the air, and the process temperature of oxidation depends on the sample preparation method. Thermal analysis is effective to detect the phase transition temperature, because the oxidation is accompanied by heat generation (exothermic effect), and the sample weight increases. The results are presented in Fig. 2.

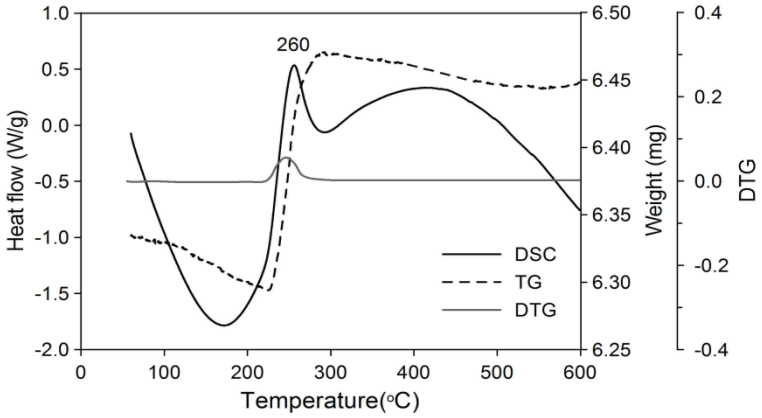

Fig. 2. DSC/DTG analysis of the product of AC electrochemical copper oxidation in a 3 wt % solution of sodium chloride at a current density of 1 A/cm^2

The sample weight increase by 2.5 wt % from the original value (2.8 wt % of the minimum weight at 224 ºC) corresponds to oxidation of copper (I) oxide to copper (II) oxide. The exothermic effect corresponding to the oxidation process is overlaid by the broad exothermic peak of crystallization and recrystallization of copper oxide (up to 600 °C). Thus, the AC copper oxidation was found to produce Cu_2O that is oxidized at lower temperatures (230−320 °C) than copper oxide prepared by conventional methods (300−400 °C) [50, 51]. The temperature of the prepared Cu_2O oxidation is reduced because the AC electrochemical copper oxidation is carried out under non-equilibrium conditions when the copper electrode potential is changed according to the frequency of the alternating current. During this synthesis, the polarities of the copper electrodes change alternatively during the electrolysis, causing the cathodic and anodic processes to alternate at the electrodes. Gaseous electrolysis products are also evolved. As a result, nanoscale particles with large internal energy storage are formed.

The high reactive ability of the particles facilitates phase transformation processes, causes the temperature of the copper oxidation to decrease and has great practical importance. This enables one to retain the specific surface area and simultaneously developed the porous structure of the phase transformation products. In addition, when preparing nanomaterials based on copper oxide, their high reactive ability contributes to more intensive interaction of the components.

Copper (I) oxide is oxidized to copper (II) oxide after aging in solution. In addition, the basic copper carbonate $Cu_2(OH)_2CO_3$ is formed.

The products of AC electrochemical metal oxidation are agglomerates. Thus, SEM analysis cannot be used to determine the size of the crystallites, which is responsible for the properties of nanomaterials when they form particles. The content of the copper compounds and crystallite sizes (coherent scattering region) were determined by full-profile X-ray diffraction patterns analysis using the “Powder Cell 2.4” program. The coherent scattering region (CSR) obtained from the Scherrer equation is 20–30 nm and do not change during aging. A feature of nanomaterials is the influence of the coherent scattering region (CSR) on the semiconductor band gap. Hence, photocatalytic and photoelectrochemical properties of nanomaterials can be adjusted by the CSR change [26].

The contents of copper compounds are shown in Fig. 3. Over time the content of copper (I) oxide decreases because of Cu_2O oxidation to CuO and $Cu_2(OH)_2CO_3$. Cu_2O content does not exceed 3 wt % after 60 days of aging.

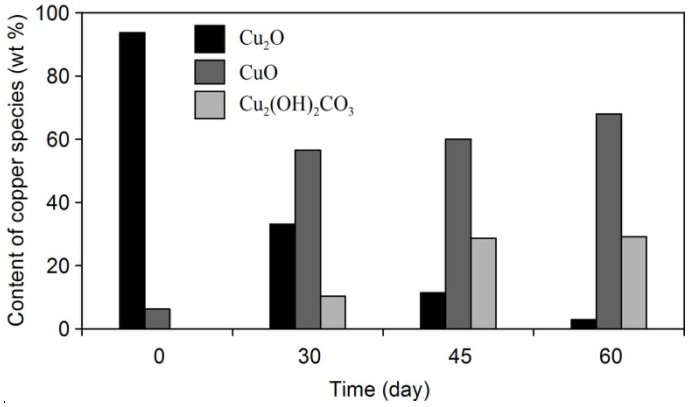

Fig. 3. The content of copper species in the products of AC electrochemical copper oxidation in a 3 wt % solution of sodium chloride at a current density of 1 A/cm^2

The aged Cu_2O phase transformation occurs as follows:

1. Cu_2O is rapidly oxidized to CuO with no $Cu_2(OH)_2CO_3$ formation for the first 30 days, because of the low CO_2 concentration.
2. Cu_2O oxidation slows down sharply when $Cu_2(OH)_2CO_3$ is actively formed during the next 15 days. It is due to the fact that basic copper carbonate formation is thermodynamically favourable under standard conditions [37].
3. CuO formation then accelerates, while the $Cu_2(OH)_2CO_3$ content does not change notably . The equilibrium of the reversible reaction of CuO transformation to $Cu_2(OH)_2CO_3$ shifts towards the reactants and as the $Cu_2(OH)_2CO_3$ content is reaching equilibrium, the CuO content rises.

Cu_2O/CuO composite can be utilized as a heterojunction photocathode for different catalytic reactions (for instance, photoelectrochemical hydrogen evolution reaction) [26].

Hydrophilicity (or hydrophobicity) of the surface depends on chemical composition and roughness. It is known that a hydrophilic (or hydrophobic) surface of bulk materials becomes superhydrophilic (or superhydrophobic) as the particle size decrease to nanoscale [52]. This can influence materials' operating performance.

CuO wettability depends on the preparation method. Thus, the dehydration way of electrolysis products is expected to influence the hydrophilicity of CuO. More hydrophobic particles will be formed after the heat treatment at residual pressure because of partial deoxygenation, whereas more hydrophilic particles will result from dehydration at atmospheric pressure after aging. Hydrophobic CuO improves the cleaning characteristics of the material and gives excellent corrosion resistance [53]. Hydrophilicity is essential for obtaining well performing catalysts and stable nanofluids.

3.2. Joint electrochemical copper and aluminum oxidation

Mixed oxides are crucial for various applications.

To prevent the degradation of the porous CuO structure for selected applications (adsorption, catalysis, chemical-looping with oxygen uncoupling, etc.), it is proposed to combine it with another oxide which has high heat resistance. One of the effective and widespread supports for this purpose, is alumina [54]. Hybrid nanofluids are a suspension of different types of nanoparticles in a base fluid. Hybrid CuO–Al_2O_3 nanofluid is reported [43] to improve the thermophysical properties of the fluid in comparison with mono nanofliuds. Likewise, hybrid metal compounds form heterojunctions that improve photocatalytic properties [27, 28].

Mixed nanopowders can be produced with AC electrolysis. Thus, joint electrochemical oxidation of copper and aluminum may be considered as the first step of a two-step method for hybrid nanofluid preparation.

The products of joint electrochemical oxidation of copper and aluminum in sodium chloride solution consist of copper (I) oxide and aluminum oxyhydroxide (boehmite) (Fig. 4). Cu_2O is conserved by drying at a residual pressure of 3−5 kPa (oxide method). Carbon-containing compounds (copper-aluminum carbonate hydroxide hydrate, Cu–Al/LDH; copper carbonate hydroxide, $Cu_2(OH)_2CO_3$) are formed during aging in solution (carbonate method). There is no stable aluminum carbonate hydroxide, therefore, the only aluminum compound is aluminum oxyhydroxide.

XRD patterns were used to determine the coherent scattering region. CSR of boehmite and copper (I) oxide obtained from the Scherrer equation are 3–4 nm and 15–20 nm, respectively. The size of the Cu_2O grains is smaller compared with those prepared by separate copper oxidation. Based on the above, the joint electrochemical oxidation of copper and aluminum improve the size distribution and stability of Cu_2O for semiconducting applications.

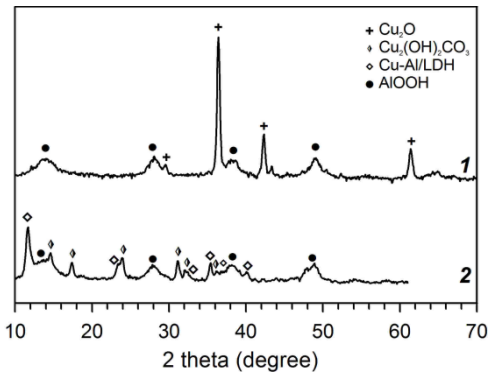

Fig. 4. XRD patterns of the products of AC electrochemical oxidation of copper and aluminum in a 3 wt % solution sodium chloride at a current density of 1 A/cm^2 after drying at 3–5 kPa (1) and carbonization in solution (2)

Copper-aluminum carbonate hydroxide hydrate has hydrotalcite-like structures of the general formula $\left[M^{II}_{1-x}M^{III}_{x}(OH)_2\right]^{x+}\cdot\left[A^{n-}_{x/n}\cdot yH_2O\right]^{x-}$ [55, 56].

Along with mixed metal oxides, Cu-Al/LDH can also be used to prepare Cu-Al LDH nanofluids applied in cooling-heat transfer devices [41].

Boehmite dehydration to alumina takes place over a wide temperature range (50−500 °C). Weight changes due to the oxidation of copper (I) oxide and hydroxocarbonate decomposition occur within the same temperature range. Thus, it is not possible to determine the loss of the sample mass (Fig. 5) due to the decomposition of different compounds, but the decomposition temperature can be accurately fixed.

The mass loss starts at about 50 ºC. It is because of the defect structure and high internal energy storage present in the products of AC electrochemical metal oxidation. According to the literature [57], it results in a phase transformation due to interaction with air-containing compounds. The IR-spectra of the products of AC-oxidation of copper and aluminum (IR-spectra not presented here) confirm the formation of carbon-containing compounds after electrolysis [58].

Copper (I) oxide, which is the part of the product of joint the AC-oxidation of copper and aluminum, is oxidized to copper (II) oxide in the same temperature range as copper (I) oxides which were formed by separate copper oxidation (230−320 °C) (Fig. 5). This is indicated by the exothermic peak in the above mentioned temperature range. Also, the weight loss in this temperature range depends on the dehydration of boehmite and the oxidation of copper (I) oxide.

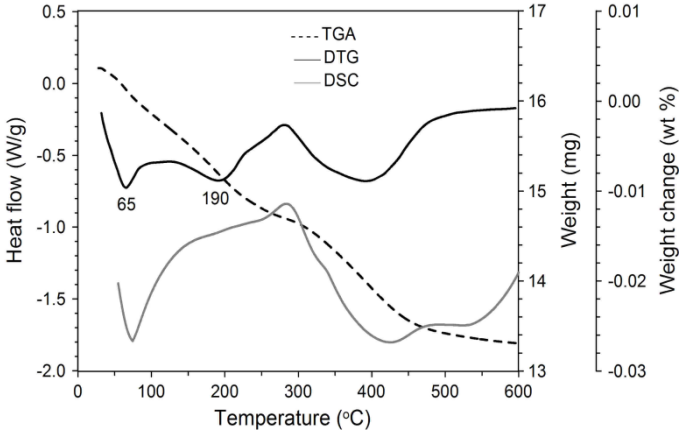

Fig. 5. DSC/DTG analysis of the products of AC electrochemical oxidation of copper and aluminum in a 3 wt % solution sodium chloride at a current density of 1 A/cm^2 after drying at 3−5 kPa

A comparison of the thermal analysis of the sample prepared by carbonate, XRD analysis of calcinated products and literature data revealed that decomposition of Cu–Al/LDH takes place in the temperature range of 110–150 °C. Thus, the layered double hydroxide derived from the products of non-equilibrium electrochemical oxidation of metals, is decomposed at lower temperatures than the LDH obtained by other methods [59]. The products of decomposition are hydrated compounds of copper and aluminum, which are converted into the oxides CuO and Al_2O_3 at high temperature .

Copper carbonate hydroxide is decomposed in two stages, each of which corresponds to an endoeffect on the DSC curve (Fig. 6).

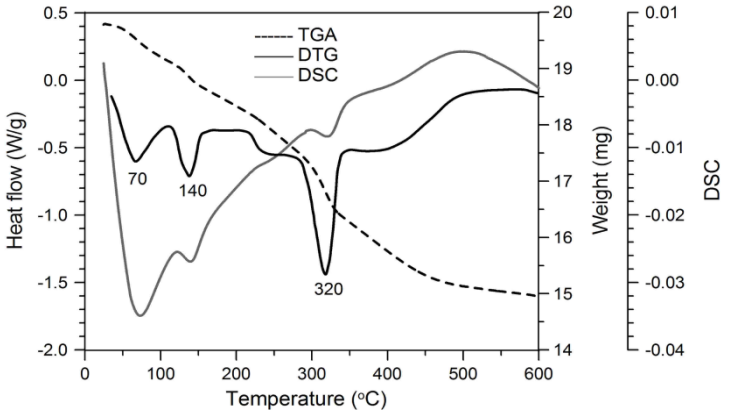

Fig. 6. DSC/DTG analysis of the products of AC electrochemical oxidation of copper and aluminum in a 3 wt % solution sodium chloride at a current density of 1 A/cm^2 after carbonization in solution

The first stage – dehydration at 155−260 °C is:

$$Cu_2(OH)_2CO_3 = CuO{\cdot}CuCO_3 + H_2O.$$

The second stage – decomposition at 260−360 °C is:

$$CuO{\cdot}CuCO_3 = CuO + CO_2.$$

The temperatures of copper carbonate hydroxide decomposition are significantly lower than ones in the literature for this process [60].

In conclusion, improvement of catalytic, photocatalytic and conductive properties of copper-containing compounds can be tailored by joint electrochemical oxidation of copper and aluminum.

3.3. Joint electrochemical copper and cadmium oxidation

There are some general patterns of the phase changes of the products of joint metal oxidation, but at the same time there are differences compared to thermal products obtained by the joint electrochemical oxidation of copper and cadmium.

X-ray analysis showed that the dry products obtained in a NaCl solution with a concentration of 3 wt % with using different current densities at the electrodes, have different compositions. Products synthesized at a current density of 1 A/cm^2 preferably contains γ–$Cd(OH)_2$, $Cu(OH)_2$, and β–$Cd(OH)_2$, CdO and Cu_2O (Fig. 7). For a current density 3 A/cm^2, predominantly Cu_2O, and also a mixture of the hydroxides γ–$Cd(OH)_2$, β–$Cd(OH)_2$ and $Cu(OH)_2$ (Fig. 8) were obtained.

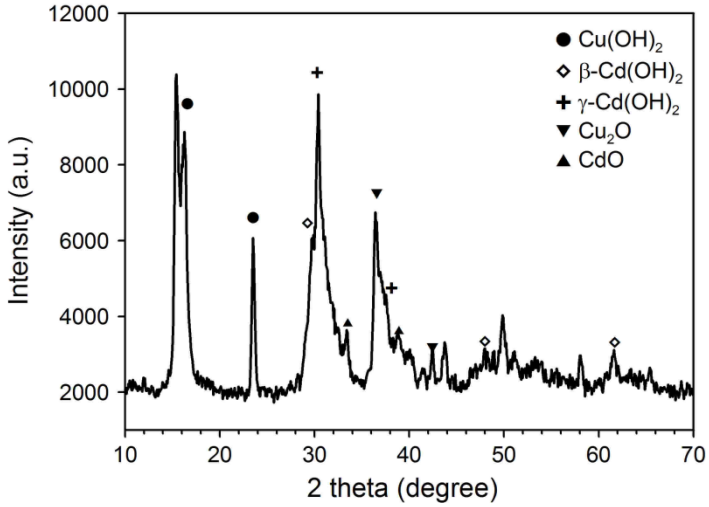

Fig. 7. XRD pattern of the product of AC electrochemical oxidation of copper and cadmium in a 3 wt % solution sodium chloride at a current density of 1 A/cm^2

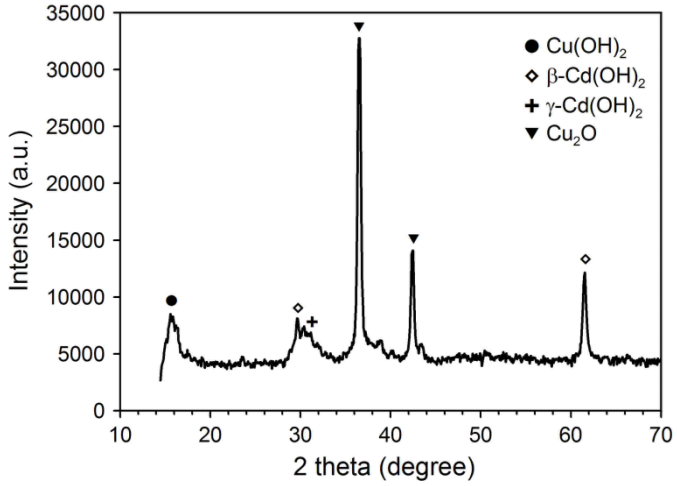

Fig. 8. XRD pattern of the product of AC electrochemical oxidation of copper and cadmium in a 3 wt % solution sodium chloride at a current density of 3 A/cm^2

Fig. 7 and 8 shows that the current density during electrolysis has a significant impact on the composition of the products formed. X-ray results are confirmed by differential thermal analysis, presented in Fig. 9 and 10.

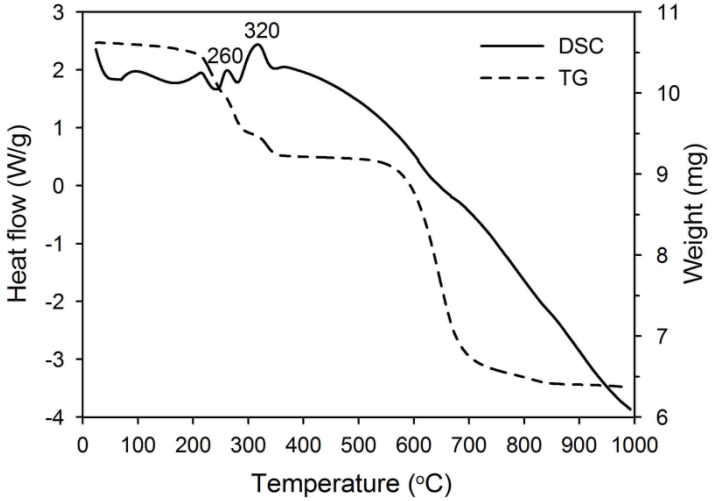

Fig. 9. DSC/DTG analysis of the product of AC electrochemical oxidation of copper and cadmium in a 3 wt % solution sodium chloride at a current density of 1 A/cm^2

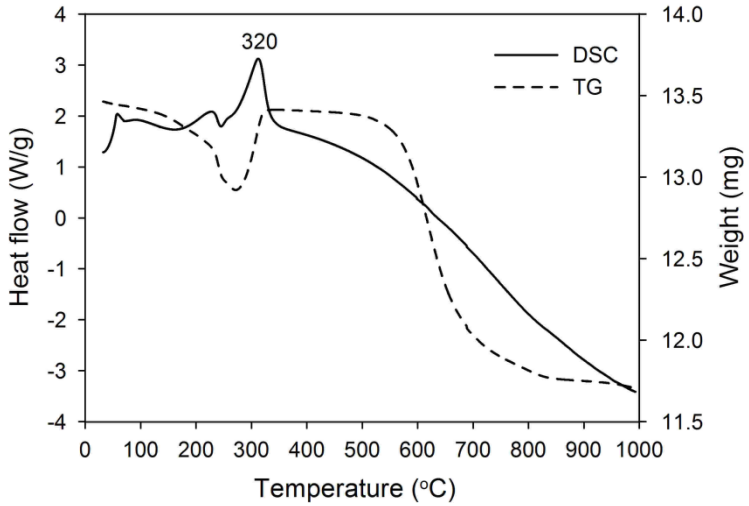

Fig. 10. DSC/DTG analysis of the product of AC electrochemical oxidation of copper and cadmium in a 3 wt % solution sodium chloride at a current density of 3 A/cm^2

Material prepared in a sodium chloride solution of 3 wt % and a current density of 1 A/cm^2 is characterized by a TGA curve having a step shape (Fig. 9). The observed thermal effects are for the processes related to dehydration, Cu_2O to CuO oxidation and dissociation of dispersed oxides, respectively. The main dehydration processes of hydroxides of cadmium and copper, occur in a temperature range of 180 to 350 °C [14]. They are accompanied by a mass loss of 12.3%. Weight loss is slowing in the range of 280–340 °C due to oxidation of Cu_2O to CuO which occurred exothermally at 320 °C. The major process in the temperature over 580 °C, accompanied by a mass decrease by 25.3 wt %, is related to the dissociation of oxides. The beginning of these effects is shifted to lower temperatures due to the dissociation process of fine oxides, mainly of CdO.

It gives a different picture DTG-DSC analysis of the product obtained at a current density of 3 A/cm^2, since it includes oxide components, mostly Cu_2O. The weight loss due to the dehydration of hydroxides of copper and cadmium (3.74 %) in the range of 180–350 °C is due to the Cu_2O to CuO oxidation process with an increase in weight of the sample compared to the original value. The exothermic oxidation effect is 2 times higher than for the product obtained at a current density of 1 A/cm^2. Further changes in the DSC and DTG curves after the temperature of 580°C reflect the dissociation of cadmium and copper oxides.

Thus, the products of electrochemical oxidation of metallic copper and cadmium with altering current is a mixture of copper oxide (I) and (II), and hydroxides of cadmium and copper having amorphous character. These substances are not converted into carbonates during aging, because the copper-cadmium layered double hydroxides do not exist.

4. Conclusion

Electrochemical copper oxidation using alternating current forms the copper (I) oxide. Its color indicates a blue shift because of its nanostructure formation. Copper (I) oxide is oxidized to copper (II) oxide during storage in solution or through atmospheric heat treatment at 260 °C. Aging of the electrolysis products in electrolyte solution causes the formation of copper carbonate hydroxide through carbon-containing compounds in air. The coherent scattering region (CSR) of all copper compounds is 20–30 nm. Joint electrochemical oxidation of copper and aluminum results in an agglomerated formation of nanosized copper (I) oxide – aluminum oxyhydroxide system, that is carbonized after aging to the copper-aluminum layered double hydroxide containing carbonate ions between the layers. SCR of copper (I) oxide is 15–20 nm, which is less than SCR after the separate copper oxidation. It was found that the AC electrolysis causes the decomposition of carbon compounds at lower temperature than ordinary methods producing LDH. Products of the joint oxidation of copper and cadmium consists of oxides and hydroxides of copper and cadmium (γ–$Cd(OH)_2$, $Cu(OH)_2$, and β–$Cd(OH)_2$, CdO and Cu_2O) that are not transformed into carbonates because there is no copper-cadmium layered double hydroxides. Joint AC oxidation of copper and aluminum does not affect the temperature of the Cu_2O oxidation, whereas electrolysis with cadmium causes the temperature to increase to 320 °C.

Further investigations will cover the extended characterizing of the products of the electrochemical metal oxidation using alternating current to develop different applications of copper-containing materials. Nanopowders are popular to create appropriate materials for catalytic and photovoltaic applications, because of the combined effect of the small grain size of AC electrolysis products, semiconductor properties of copper- and cadmium-species, and enhanced heat and mass transfer due to increased internal energy contained in the nanopowders. Preparation of stable metal oxide nanofluids by a two-step method using different base fluids, as well as the investigation of nanofluid performance in different applications, will be also performed and reported in a follow-up paper.

Acknowledgements

The research is carried out at Tomsk Polytechnic University. The research is funded from Tomsk Polytechnic University Competitiveness Enhancement Program grant, Project Number TPU CEP_NOC N.M. Kizhnera-188/2020.

Literature

[1] I. Borovinskaya, A. Gromov, E. Levashov, Y. Maksimov, A. Mukasyan, A. Rogachev, Concise Encyclopedia of Self-Propagating High-Temperature Synthesis. 1st Edition, 2017. https://www.elsevier.com/books/concise-encyclopedia-of-self-propagating-high-temperature-synthesis/borovinskaya/978-0-12-804173-4

[2] T. Friščić, C. Mottillo, H.M. Titi, Mechanochemistry for Synthesis, 2019. https://doi.org/10.1002/anie.201906755

[3] B. Graves, S. Engelke, C. Jo, H.G. Baldovi, J. Verpilliere, M. Volder, A. Boies, Plasma production of nanomaterials for energy storage: continuous gas-phase synthesis of metal oxide CNT materials via a microwave plasma, Nanoscale. 12 (2020) 5196–5208, https://doi.org/10.1039/C9NR08886E.

[4] Y.A. Kotov, Electric explosion of wires as a method for preparation of nanopowders. Journal of Nanoparticle Research, 5 (2003) 539–550, URL: https://link.springer.com/article/10.1023/B:NANO.0000006069.45073.0b

[5] A. Pustovalov, V. An, J.C. Kim, Optimal modes for the fabrication of aluminum nanopowders by the electrical explosion of wires. Advances in Materials Science and Engineering, 2017. https://doi.org/10.1155/2017/1738949

[6] V. An , B. Liu, Synthesis of multilevel ZnS/ZnO nanostructures by electrospark erosion, Chalcogenide Letters, 12 (2015) 639–644, URL: http://www.chalcogen.ro/639_An.pdf

[7] Advanced Ceramic Processing. Edited by Adel Mohamed. InTech; 2015.

[8] A. Zubairu, A.S.B. Gimba, B. Gutti, A. Audu, Potentiostatic Electro-Deposition of *p-n* Homo-Junction Cuprous Oxide Solar Cells, Energy and Power. 10 (2020) 20–25, doi: 10.5923/j.ep.20201001.03.

[9] A.F. Dresvyannikov, E.V. Petrova, A.I. Khairullina, Electrochemical Synthesis and Physicochemical Properties of Nanostructured Al_2O_3–ZrO_2–MgO Oxide Systems, Protection of Metals and Physical Chemistry of Surfaces, 56 (2020) 89–93, https://doi.org/10.1134/S2070205120010062.
[10] E. Musella, I. Gualandi, E. Scavetta, A. Rivalta, E. Venuti, M. Christian, V. Morandi, Angelo Mullaliu, M. Giorgetti, D. Tonelli, Newly developed electrochemical synthesis of Co-based layered double hydroxides: toward noble metal-free electro-catalysis, J. Mater. Chem. A. 7 (2019) 11241–11249. https://doi.org/10.1039/C8TA11812D.
[11] N.F. Atta, A. Galal, E.H. El-Ads, Perovskite Nanomaterials – Synthesis, Characterization, and Applications, in: Perovskite Materials, IntechOpen, 2016. https://doi.org/10.5772/61280.
[12] V.V. Korobochkin, M.A. Balmashnov, D.A. Gorlushko, N.V. Usoltseva, V.V. Bochkareva, Phase Composition and Pore Structure of Nanoparticulate Tin Oxides Prepared by AC Electrochemical Synthesis. Inorg. Mater. 49 (2013) 993–999. https://doi.org/10.1134/S0020168513100051
[13] N.V. Usoltseva, V.V. Korobochkin, M.A. Balmashnov, A.S. Dolinina, Solution transformation of the products of AC electrochemical metal oxidation. Procedia Chemistry. 15 (2015) 84–89. https://doi.org/10.1016/j.proche.2015.10.013
[14] A.S. Dolinina, V.V. Korobochkin, N.V. Usoltseva, S.E. Pugacheva, M.V. Popov, The porous structure of copper-cadmium oxide system prepared by AC electrochemical synthesis. Procedia Chemistry. 15 (2015) 143–147. https://doi.org/10.1016/j.proche.2015.10.023
[15] E. Gomaa, A. Negm, M. Tahoon, Study of redox behavior of Cu(II) and interaction of Cu(II) with lysine in the aqueous medium using cyclic voltammetry, Eur. J. Chem. 7 (2016) 341–346. https://doi.org/10.5155/eurjchem.7.3.341-346.1471.
[16] A. Demin, E. Gorbova, A. Brouzgou, A. Volkov, P. Tsiakaras, Sensors based on solid oxide electrolytes, in: M.L. Faro (Ed.) Solid Oxide-Based Electrochemical Devices: Advances, Smart Materials and Future Energy Applications, Academic Press, 2020, pp. 167–215. https://doi.org/10.1016/B978-0-12-818285-7.00006-X.
[17] E.Yu. Pikalova, V.A. Sadykov, E.A. Filonova, N.F. Eremeev, E.M. Sadovskaya, S.M. Pikalov, N.M. Bogdanovich, J.G. Lyagaeva, A.A. Kolchugin, L.B. Vedmid', A.V. Ishchenko, V.B. Goncharov. Structure, oxygen transport properties and electrode performance of Ca-substituted Nd_2NiO_4. Solid State Ionics. 335 (2019) 53–60. https://doi.org/10.1016/j.ssi.2019.02.012.
[18] M.A. San Pio, F. Sabatino, F. Gallucci, M. van Sint Annaland, Importance of spinel reaction kinetics in packed-bed chemical looping combustion using a CuO/Al_2O_3 oxygen carrier, Chem. Eng. J. 334 (2018) 1905–1916. https://doi.org/10.1016/j.cej.2017.11.138.
[19] X.H. Zhou, K.H. Song, Z.H. Li, W.M. Kang, H.R. Ren, K.M. Su, M. L. Zhang, B.W. Cheng, The excellent catalyst support of Al_2O_3 fibers with needle-like mullite structure and HMF oxidation into FDCA over CuO/Al_2O_3 fibers, Ceramics International. 45 (2019) 2330–2337, Ceramics International 45 (2019) 2330–2337.
[20] Chao-Lung Chiang, Kuen-Song Lin, Preparation and Characterization of CuO-Al_2O_3 Catalyst for Dimethyl Ether Production via Methanol Dehydration, Int. J. Hydrog. Energy. 42 (2017) 23526–23538. https://doi.org/10.1016/j.ijhydene.2017.01.063
[21] P. Sriprom, S. Neramittagapong, C. Lin, K. Wantala, A. Neramittagapong, N. Grisdanurak, Optimizing chemical oxygen demand removal from synthesized wastewater containing lignin by catalytic wet-air oxidation over CuO/Al_2O_3 catalysts. J. Air Waste Manag. Assoc. 65 (2015) 828–836. https://doi.org/10.1080/10962247.2015.1023908
[22] N.Wu, Q.Liu, Y. Ding, W. Fang, Y. He, J. Li, Ch. Jiang, Yu. Wang, CuO/Al_2O_3 Catalyst Preparation Conditions for Removal of Nitrobenzene by Heterogeneous Fenton-Like System, Pol. J. Environ. Stud. 29 (2020) 1909–1917. https://doi.org/10.15244/pjoes/109276.
[23] A. Mujtaba, N.K. Janjua, Fabrication and Electrocatalytic Application of $CuO@Al_2O_3$ Hybrids, J. Electrochem. Soc. 162 (2015) H328–H337. https://doi.org/10.1149/2.0351506jes
[24] Ma Rui, Liu Guangmin, Feng Sihui, Qiu Xiaoyu, Zhang Yanqing, Xia Shumei, Xue Jianliang, Optimization and Effects of Catalytic Ozonation of Actual Phenolic Wastewater by CuO/Al_2O_3, China Petroleum Processing and Petrochemical Technology. 21 (2019) 74–80.
[25] Q.L. Zhang, Y. Dong, L. Cui, Simultaneous removal of SO_2 and NO from flue gas using CeO_2 promoted CuO/γ-Al_2O_3 catalysts, IOP Conf. Series: Earth and Environmental Science. 508 (2020) 012139, doi:10.1088/1755-1315/508/1/012139.
[26] Yang Yang, Di Xu, Qingyong Wu & Peng Diao, Cu_2O/CuO Bilayered Composite as a High-Efficiency Photocathode for Photoelectrochemical Hydrogen Evolution Reaction, Scienfitic reports, 6 (2016) Article number 35158, https://doi.org/10.1038/srep35158
[27] J.F. Han, X. Zong, X. Zhou, C. Li, Cu_2O/CuO photocathode with improved stability for photoelectrochemical water reduction, RSC Advances, 5 (2015) 10790–10794, https://doi.org/10.1039/c4ra13896a
[28] Wei Li, Mingyang Li, Shilei Xie, Teng Zhai, Minghao Yu, Chaolun Liang, Xingwang Ouyang, Xihong Lu, Haohua Li, Yexiang Tong, Improving the photoelectrochemical and photocatalytic performance of CdO nanorods with CdS decoration, CrystEngComm, 15 (2013) 4212–4216, https://doi.org/10.1039/c3ce40092a
[29] N. Ali, J.A. Teixeira, A. Addali, A Review on Nanofluids: Fabrication, Stability, and Thermophysical Properties, Journal of Nanomaterials. (2018) Article ID 6978130, https://doi.org/10.1155/2018/6978130.
[30] T. Arunkumara, K. Raj, D. Denkenberger, R. Velraj, Heat carrier nanofluids in solar still – A review, Desalination and Water Treatment. 130 (2018) 1–16, https://doi.org/10.5004/dwt.2018.22972.

[31] M. Sheikholeslami, R. Haq, A. Shafee, Z. Li, Y.G. Elaraki, I. Tlili, Heat transfer simulation of heat storage unit with nanoparticles and fins through a heat exchanger, International Journal of Heat and Mass Transfer. 135 (2019) 470–478, https://doi.org/10.1016/j.ijheatmasstransfer.2019.02.003.
[32] E. Bellos, C. Tzivanidis, A review of concentrating solar thermal collectors with and without nanofluids, Journal of Thermal Analysis and Calorimetry. 135 (2019) 763–786, https://doi.org/10.1007/s10973-018-7183-1
[33] A. Ahmed, H. Baig, S. Sundaram, T.K. Mallick**,** Use of Nanofluids in Solar PV/Thermal Systems, International Journal of Photoenergy. (2019) Article ID 8039129, https://doi.org/10.1155/2019/8039129.
[34] M. Sheikholeslami, S.A. Farshad, A. Shafee, H. Babazadeh, Numerical modeling for nanomaterial behavior in a solar unit analyzing entropy generation, Journal of the Taiwan Institute of Chemical Engineers. 000 (2020) 1–15, https://doi.org/10.1016/j.jtice.2020.06.005.
[35] M. Sheikholeslami, M. Jafaryar, E. Abohamzeh, A. Shafeed, H. Babazadeh, Energy and entropy evaluation and two-phase simulation of nanoparticles within a solar unit with impose of new turbulator, Sustainable Energy Technologies and Assessments. 39 (2020) 100727, https://doi.org/10.1016/j.seta.2020.100727.
[36] M. Sheikholeslami, M. Jafaryar, A. Shafee, H. Babazadeh, Acceleration of discharge process of clean energy storage unit with insertion of porous foam considering nanoparticle enhanced paraffin, Journal of Cleaner Production. 261 (2020) 121206, https://doi.org/10.1016/j.jclepro.2020.121206.
[37] N.B. Tanvir, O. Yurchenko,Ch. Wilbertz, G. Urban, Investigation of CO_2 reaction with copper oxide nanoparticles for room temperature gas sensing, J. Mater. Chem. A, 4 (2016) 5294–5302, https://doi.org/10.1039/c5ta09089j
[38] M. Sheikholeslami, B.Rezaeianjouybari, M. Darzi, A. Shafee, Z. Li, T.K. Nguyen, Application of nano-refrigerant for boiling heat transfer enhancement employing an experimental study, International Journal of Heat and Mass Transfer 141 (2019) 974–980, https://doi.org/10.1016/j.ijheatmasstransfer.2019.07.043.
[39] S. Amalraj, P.A. Michael, Synthesis and characterization of Al_2O_3 and CuO nanoparticles into nanofluids for solar panel applications, Results in Physics. 15 (2019) 102797, https://doi.org/10.1016/j.rinp.2019.102797
[40] M. Sheikholeslami, R. Haq, A. Shafee, Z. Li, Y.G. Elaraki, I. Tlili, Heat transfer simulation of heat storage unit with nanoparticles and fins through a heat exchanger, International Journal of Heat and Mass Transfer. 135 (2019) 470–478, https://doi.org/10.1016/j.ijheatmasstransfer.2019.02.003.
[41] M. Y.A. Shdaifat, R. Zulkifli, K. Sopian, A.A. Salih, Thermal and Hydraulic Performance of CuO/Water Nanofluids: A Review, Micromachines. 11 (2020) 416, doi: https://doi.org/10.3390/mi11040416.
[42] E.C. Okonkwo, I. Wole‐Osho, I.W. Almanassra, Y.M. Abdullatif, T.Al. Ansari, An updated review of nanofluids in various heat transfer devices, Journal of Thermal Analysis and Calorimetry. (2020), https://doi.org/10.1007/s10973-020-09760-2.
[43] S. Senthilraja, K. Vijayakumar, R. Gangadevi, A comparative study on thermal conductivity of Al_2O_3/water, CuO/water and Al_2O_3–CuO/water nanofluids, Digest Journal of Nanomaterials and Biostructures. 10 (2015) 1449–1458, https://pdfs.semanticscholar.org/3ce1/ef37bad0e742fdeff9fcef6de0c72b19023a.pdf
[44] A.S. Murugesh, M.R.V. T. Kumar, Enhancing Heat Transfer Rate of Heat Exchanger using Cadmium Oxide Nanofluid, International Journal for Scientific Research & Development. 5 (2017) 1278–1281, http://www.ijsrd.com/articles/IJSRDV5I20922.pdf
[45] M.S.H. Akash, K. Rehman, Introduction to Thermal Analysis, in: Essentials of Pharmaceutical Analysis, Springer, Singapore, (2020) 195–198, https://doi.org/10.1007/978-981-15-1547-7_16.
[46] Mansfield E. Recent advances in thermal analysis of nanoparticles: methods, models and kinetics, in: Modeling, Characterization, and Production of Nanomaterials. Edited by V.K. Tewary, Y. Zhang, Woodhead Publishing, (2015) 167–178. https://doi.org/10.1016/B978-1-78242-228-0.00006-5.
[47] C.F. Holder, R.E. Schaak**,** Tutorial on Powder X‐ray Diffraction for Characterizing Nanoscale Materials, ACS Nano. 7 (2019) 7359–7365. https://doi.org/10.1021/acsnano.9b05157
[48] B.A. Gizhevskiĭ, Yu. P. Sukhorukov, A. S. Moskvin, N. N. Loshkareva, E. V. Mostovshchikova, A. E. Ermakov, E. A. Kozlov, M. A. Uĭmin, V. S. Gaviko, Anomalies in the optical properties of nanocrystalline copper oxides CuO and Cu_2O near the fundamental absorption edge, J. Exp. Theor. Phys+. 102 (2016) 297–302. https://doi.org/10.1134/S1063776106020105.
[49] Handbook of Nanostructured Anodic Metal Oxides. 1st ed., Grzegorz Sulka (Ed.), Elsevier, USA, 2020. https://www.elsevier.com/books/nanostructured-anodic-metal-oxides/sulka/978-0-12-816706-9.
[50] Y. Wang, S. Lany, J. Ghanbaja, Y. Fagot-Revurat, Y. P. Chen, F. Soldera, D. Horwat, F. Mücklich, J.F. Pierson, Electronic structures of Cu_2O, Cu_4O_3, and CuO: A joint experimental and theoretical study. Phys. Rev. B: Condensed Matter and Materials Physics, American Physical Society, 94 (2016) 245418. https://doi.org/10.1103/PhysRevB.94.245418.
[51] Y. Zhu, K. Mimura, M. Issiki, Oxidation Mechanism of Cu_2O to CuO at 600−1050 °C, Oxid. Met. 62 (2004) 207–222. https://doi.org/10.1007/s11085-004-7808-6.
[52] D. Ahmad, I. van den Boogaert, J.Miller, R. Presswell, H. Jouhara, Hydrophilic and hydrophobic materials and their applications, Energy sources, part a: recovery, utilization, and environmental effects. 40 (2018) 2686–2725, https://doi.org/10.1080/15567036.2018.1511642
[53] W. Dou, J. Wu, T. Gu, P. Wang, D. Zhang, Preparation of super-hydrophobic micro-needle CuO surface as a barrier against marine atmospheric corrosion, Corrosion Science. 131 (2018) 156–163, https://doi.org/10.1016/j.corsci.2017.11.012.

[54] M.A. San Pio, M. Martini, F. Gallucci, I. Roghair, M. van Sint Annaland, Kinetics of CuO/SiO_2 and CuO/Al_2O_3 oxygen carriers for chemical looping combustion, Chemical Engineering Science, 175 (2018) 56–71, https://doi.org/10.1016/j.ces.2017.09.044
[55] Handbook of Clay Science, in: Developments in Clay Science. F. Bergaya, B.K.G. Theng, G. Lagaly (Eds.), Amsterdam, Elsevier Ltd. 2006.
[56] M. Zhao, Q. Zhao, B. Li, H. Xue, H. Pang, C. Chen, Recent progress in layered double hydroxide based materials for electrochemical capacitors: design, synthesis and performance, Nanoscale, 9 (2017) 15206–15225, https://doi.org/10.1039/c7nr04752e.
[57] N.T.T. Ha, V.T.M. Hue, B.C. Trinh, N.N. Ha, L.M. Cam, Study on the Adsorption and Activation Behaviours of Carbon Dioxide over Copper Cluster (Cu-4) and Alumina-Supported Copper Catalyst (Cu-4/Al_2O_3) by means of Density Functional Theory, Journal of Chemistry, (2019) Article ID 4341056, https://doi.org/10.1155/2019/4341056
[58] N.V. Usoltseva, V.V. Korobochkin, A.S. Dolinina, A.M. Ustyugov, Infrared spectra Investigation of CuO-Al_2O_3 Precursors Produced by Electrochemical Oxidation of Copper and Aluminum Using Alternating Current, Key Engineering Materials. 712 (2016) 65–70, https://doi.org/10.4028/www.scientific.net/KEM.712.65
[59] A.A. Sertsova, E.N. Subcheva, E.V. Yurtov, Synthesis and study of structure formation of layered double hydroxides based on Mg, Zn, Cu, and Al, Russian Journal of Inorganic Chemistry, 60 (2015) 23–32, doi: https://doi.org/10.1134/S0036023615010167.
[60] G. Zhu, H. Xu, Y. Xiao, Y. Liu, A. Yuan, X. Shen, Facile Fabrication and Enhanced Sensing Properties of Hierarchically Porous CuO Architectures. ACS Appl. Mater. Interfaces. 4 (2012) 744−751, dx.doi.org/10.1021/am2013882.